

A new OSL chronology for dust accumulation in the last 130,000 yr for the Chinese Loess Plateau

Y.C. Lu^{a,b,*}, X.L. Wang^a, A.G. Wintle^c

^a SKLLQG, Institute of Earth Environment, Chinese Academy of Sciences, Xi'an 710075, China

^b SKLED, Institute of Geology, China Seismological Bureau, Beijing 100029, China

^c Institute of Geography and Earth Sciences, University of Wales, Aberystwyth, SY23 3DB, UK

Received 26 July 2005

Available online 13 October 2006

Abstract

A sensitivity-corrected Multiple Aliquot Regenerative-dose protocol has been developed for fine-grained quartz OSL dating of Chinese loess. Its reliability has been assessed on the basis of the methodology and by dating reference samples of known age close to the transition from the last interglacial paleosol (S_1) to the last glacial loess (L_1), which corresponds to the Marine Oxygen Isotope Stage (MIS) 5/4 transition. On the basis of the fine-grained quartz OSL-age estimates for 33 loess samples from the upper part of the Luochuan profile, a detailed chronostratigraphy of continuous dust accumulation in the past 130 ka has been proposed. Changes in the accumulation rate occurred during the last glacial period (MIS 4 to MIS 2); unexpectedly, high accumulation rates were found in the weakly developed $L_{1-2(S)}$ paleosol of the last interstadial (MIS 3), rather than in the classic L_{1-1} and L_{1-3} loess of the cold-dry glacial condition (MIS 2 and 4). The OSL ages show some disagreement with the previous numerical chronology for the loess–paleosol sequence based on correlation of variations in grain size with sedimentation rate; the latter method resulted in an almost constant accumulation rate from 72 to 12 ka.

© 2006 University of Washington. All rights reserved.

Keywords: Fine-grained quartz; OSL; Sensitivity-corrected MAR protocol; Chinese loess

Introduction

The well-known Luochuan loess–paleosol sequence is very important for Chinese loess research, and it has acted as a key section for reconstructing the paleoclimate on the continent during the last glacial–interglacial cycle (e.g., An and Lu, 1984; Liu, 1985; Porter and An, 1995; An and Porter, 1997; Rousseau and Wu, 1997; Xiao et al., 1999; Bronger, 2003). A reliable chronology is critical for the calculation of rates of dust deposition, and also for paleoclimatic reconstruction in the late Quaternary. Recently, numerical chronologies have been obtained by using the percentage of coarse silt fraction ($>40\ \mu\text{m}$) (Porter and An, 1995) or the median diameter (Xiao et al., 1999) of the chemically isolated quartz fraction as a

proxy for dust flux, ages being assigned based on an accumulation rate model that is linked to the SPECMAP time scale (Porter and An, 1995; Xiao et al., 1999). This approach is usually named the “grain-size model” for Chinese loess (Porter and An, 1995); the uncertainty range over the last glacial–interglacial period is ca. 1000–3000 yr (Porter, 2001). However, an independent absolute chronology is vital for Chinese loess deposited in the past 130 ka. Lu et al. (1987, 1988) were the first to set up a thermoluminescence (TL) chronology for Chinese loess near Xi'an and Beijing, and Forman (1991) dated a section near Luochuan on the Chinese Loess Plateau. These studies provided a rough chronology for Chinese loess formed in the late Quaternary. Until 1996, most of the luminescence age estimates for Chinese loess had been obtained by multiple aliquot thermoluminescence (TL), and some by infrared-stimulated luminescence (IRSL), dating methods applied to polymineral fine grains (Lu et al., 1987, 1988, 1999; Forman, 1991; Musson et al., 1994; Frechen, 1999; Zhao, 2003). The

* Corresponding author. Fax: +86 29 8832 0456.

E-mail address: yeh.lu@263.net (Y.C. Lu).

precision and accuracy of TL and IRSL ages beyond 50 ka has been questioned (e.g., Wintle, 1990; Zhou et al., 1995; Prescott and Robertson, 1997).

However, luminescence dating has undergone many innovations in methodology in the past decades, especially with the development of Optically Stimulated Luminescence (OSL) dating (Huntley et al., 1985). For obtaining precise OSL ages that could be used to construct a high-resolution chronology, the regeneration method is a good choice; in this method, the natural luminescence is compared with that resulting from laboratory irradiation. Thus, the precise form of the growth curves and the mathematical function selected for fitting the data are unimportant and the equivalent dose (D_e) is obtained by interpolation; this results in higher precision for D_e determination (Wintle, 1997; Aitken, 1998). The critical disadvantage is that if any sensitivity changes occur between measurements of the natural and regenerative OSL signals, the age obtained will be inaccurate. Zhou and Wintle (1994) and Zhou et al. (1995) considered that most of the TL age estimates obtained by the regeneration method on polymineral loess samples were underestimated, and they attributed this mainly to sensitivity changes induced by the laboratory optical bleaching prior to laboratory irradiation.

In a preliminary study of a single sample of Chinese loess, Zhou and Shackleton (2001) concluded that using a test dose OSL response for monitoring sensitivity changes in the Single-Aliquot Regenerative-dose (SAR) procedure (Murray and Wintle, 2000) was a potentially useful approach. However, from the early saturation levels shown by the sensitivity-corrected dose–response curves, they concluded that it would not be possible to date beyond 55 ka in Chinese loess. These sensitivity monitoring measurements can also be used for inter-aliquot normalization in the construction of standardized dose–response curves (Roberts and Duller, 2004). Using such measurements, we have developed a sensitivity-corrected Multiple Aliquot Regenerative-dose (MAR) method for loess, subsequently referred to as the sensitivity-corrected MAR protocol. After each natural and regenerative OSL (L_x) measurement, a test dose OSL response (T_x) is measured to compensate for differences in luminescence production during the measurement of the quartz OSL signals. The growth of the normalized luminescence (L_x/T_x) for the regeneration doses is used to determine the D_e value for the natural value (L_N/T_N). After estimating the reliability of this sensitivity-corrected MAR protocol, we use it to set up an independent chronology for the Luochuan loess–paleosol section in the last glacial–interglacial cycle, and the closely spaced OSL ages were used to evaluate the rate of dust accumulation in the last glacial period.

Sample site and sample preparation

At Luochuan (35°45'N, 109°25'E), the exposed sediments are composed of more than 30 loess–paleosol alternations with a total thickness of 135 m (Liu, 1985). These sediments have been subjected to extensive multidisciplinary studies on stratigraphy and paleoclimate reconstruction (e.g., Liu, 1985; Kukla, 1987; Kukla et al., 1988; Kukla and An, 1989; An et al.,

1990; Forman, 1991; Porter and An, 1995; An and Porter, 1997; Rousseau and Wu, 1997; Xiao et al., 1999; Bronger, 2003). In the current study, 33 samples from the upper 13 m, made up of 2 samples from L_2 , 7 samples from the paleosol unit S_1 , 21 samples from L_1 and S_0 and 3 samples from the recent loess (L_0) (Fig. 5 and Table 1), were obtained by hammering stainless-steel tubes into cleaned pit walls at the Heimugou section, Luochuan.

Following the laboratory procedures for Chinese loess (Lu et al., 1988; Forman, 1991), the samples were extracted under subdued red light and pretreated with 30% HCl and 30% H_2O_2 to remove the carbonates and organic material, respectively. Then the fine silt (4–11 μm) was obtained using sedimentation procedures based on Stokes' Law. These polymineral fine grains were immersed in hydrofluorosilicic acid, H_2SiF_6 (30%), for 3 days in an ultrasonic bath to obtain the fine-grained quartz component. The purity of the isolated quartz was checked by IR stimulation. The first 1-s IRSL signal (with a laboratory regenerative dose of 19.2 Gy and preheat condition of 260°C for 10 s) was less than 200 counts/s (most of them less than 100 counts/s) after subtracting the instrumental background; this indicates a dominance of quartz, with no significant OSL signal contribution from feldspar (Wang et al., 2006). In addition, for some samples X-ray diffraction was applied in order to confirm the lack of feldspar.

Instruments and measurements

All measurements were performed using a Daybreak 2200 automated OSL reader equipped with a combined blue (470 ± 5 nm) and infrared (880 ± 80 nm) LED OSL unit, two $^{90}\text{Sr}/^{90}\text{Y}$ beta sources (0.19 and 0.157 Gy/s) and an Am-241 alpha source ($0.062 \mu\text{m}^{-2} \text{s}^{-1}$) for irradiations. All luminescence measurements were made at 125°C for 50 s with both IR and blue stimulation powers at $\sim 45 \text{ mW/cm}^2$. Luminescence emissions were detected by an EMI 9235QA photomultiplier tube and two 3 mm U-340 glass filters. For D_e calculation, the first 5-s integral of the OSL decay curve was used after subtracting that of the last 5 s. Bleaching is provided by a solar simulator (SOL2) and the exposure time was 180 s.

D_e determination by the sensitivity-corrected MAR protocol

Description of the sensitivity-corrected MAR protocol

As mentioned in the introduction, the OSL response (T_i) to a test dose is used to correct for sensitivity changes caused by the bleaching prior to the regeneration doses and by any thermal treatment prior to the measurement of L_i , as well as to normalize for the differences (e.g., due to sample mass) between the different aliquots. Figure 1 presents the OSL decay curves, both L_i (Figs. 1a and b) and T_i (Figs. 1c and d) for two samples and sensitivity-corrected (L_i/T_i) dose–response curves (Figs. 1e and f) for D_e determination using the sensitivity-corrected MAR protocol. Bleaching was with the SOL2 for 180 s (shown as SL in text in Figs. 1a and b). For D_e estimation, the corrected OSL

Table 1
Summary of dosimetry and OSL ages at Luochuan Heimugou section, with the positions of the transitions based on the climato-stratigraphy of An and Lu (1984)

Lab No.	Depth (m)	U (ppm)	Th (ppm)	K (%)	Water content (%)	Alpha coefficient	Dose rate (Gy/ka)	D_c (Gy)	OSL age (ka)	Transition
IEE208	0.1	2.19±0.08	11.50±0.25	1.86	15±2	0.040	3.48±0.11	3.6±0.2	1.0±1	
IEE209	0.3	2.34±0.09	12.20±0.27	1.90	15±2	0.039	3.60±0.12	3.0±0.4	0.8±0.1	
IEE210	0.5	2.46±0.10	13.10±0.29	1.91	18±2	0.039	3.57±0.12	4.3±0.6	1.2±0.02	
IEE211	0.8	2.38±0.10	13.50±0.30	2.07	18±2	0.035	3.66±0.12	29.2±0.6	8.0±0.3	
IEE213	1.4	2.21±0.09	11.40±0.25	1.51	18±2	0.036	2.97±0.10	34.6±0.3	11.7±0.4	L ₁₋₁ /S ₀
IEE214	1.8	2.11±0.08	11.00±0.24	1.73	15±2	0.037	3.22±0.11	51.9±1.2	16.1±0.7	
IEE215	2.0	2.39±0.10	11.60±0.26	1.69	15±2	0.048	3.44±0.12	79.8±2.4	23.2±1.1	
IEE216	2.3	2.30±0.09	12.60±0.28	1.79	15±2	0.045	3.55±0.12	93.5±0.12	26.4±1.1	
IEE217	2.6	2.28±0.09	12.50±0.28	1.79	15±2	0.038	3.45±0.12	96.5±3.2	28.0±1.3	
IEE218	3.0	2.17±0.09	11.80±0.26	1.86	15±2	0.053	3.57±0.12	113±1.5	31.6±1.1	L _{1-2(s)} /L ₁₋₁
IEE219	3.5	2.31±0.09	12.20±0.27	2.03	20±2	0.035	3.35±0.12	110±1.5	32.8±1.2	
IEE220	4.0	2.06±0.08	11.70±0.26	2.02	20±2	0.047	3.34±0.11	124±2.8	37.2±1.5	
IEE221	4.5	2.30±0.09	12.70±0.28	2.00	20±2	0.054	3.39±0.12	135±3.8	39.9±1.8	
IEE222	5.0	2.31±0.09	12.70±0.28	2.00	20±2	0.054	3.54±0.13	151±7.0	42.5±2.5	
IEE223	5.5	2.22±0.09	12.20±0.27	1.94	20±2	0.044	3.32±0.12	168±6.4	50.7±2.6	
IEE224	6.0	2.18±0.09	12.10±0.27	2.03	20±2	0.065	3.57±0.13	189±3.8	53.0±2.2	
IEE225	6.5	2.35±0.09	12.10±0.27	2.02	20±2	0.061	3.57±0.13	190±2.0	53.1±2.0	
IEE226	7.0	2.33±0.09	12.30±0.27	1.96	20±2	0.043	3.34±0.12	189±5.4	56.5±2.6	
IEE227	7.5	2.39±0.10	12.40±0.27	1.89	20±2	0.045	3.33±0.12	190±7.2	57.2±3.0	L ₁₋₃ /L _{1-2(s)}
IEE273	7.7	2.23±0.12	10.75±0.25	1.82	15±2	0.055	3.42±0.12	208±11	60.8±3.8	
IEE272	8.0	2.43±0.13	12.01±0.26	1.84	15±2	0.045	3.50±0.13	214±15	61.2±4.8	
IEE228	8.5	2.40±0.10	11.40±0.25	1.88	15±2	0.056	3.59±0.13	232±4.4	64.6±2.6	
IEE229	8.7	2.37±0.09	12.10±0.27	1.92	25±2	0.048	3.10±0.11	221±6.8	71.1±3.4	
IEE230	9.0	2.57±0.10	12.50±0.28	1.97	25±2	0.057	3.31±0.12	233±0.7	70.4±2.6	
IEE232	9.5	2.55±0.10	13.80±0.30	2.01	25±2	0.052	3.35±0.16	270±12	80.6±5.3	S ₁ /L ₁₋₃
IEE233	9.8	2.49±0.10	13.80±0.30	2.10	20±2	0.039	3.48±0.16	281±14	80.8±5.5	
IEE234	10.0	2.65±0.11	15.00±0.33	2.08	20±2	0.045	3.63±0.17	303±2	83.6±3.9	
IEE270	10.6	2.48±0.14	15.50±0.34	2.09	20±2	0.039	3.51±0.16	341±16	97.3±6.5	
IEE269	11.0	2.28±0.15	14.18±0.13	2.06	20±2	0.049	3.43±0.16	322±18	94.0±6.8	
IEE268	11.5	2.72±0.15	13.45±0.30	2.07	20±2	0.054	3.48±0.16	354±11	102±5.8	
IEE267	11.9	2.79±0.14	14.83±0.33	2.04	20±2	0.038	3.40±0.16	390±6	115±5.7	
IEE266	12.3	2.61±0.14	13.07±0.29	1.96	20±2	0.040	3.24±0.15	409±18	126±8.1	L ₂ /S ₁
IEE263	12.9	2.86±0.14	12.22±0.27	1.82	20±2	0.041	3.16±0.15	397±11	126±6.0	

intensity (L_i/T_i) is used. Generally, more than three aliquots are measured to determine the natural OSL intensity, and five aliquots to construct the dose–response curve that brackets the natural OSL intensity. The preheating prior to measurement of L_i was chosen to be 260°C for 10 s on the basis of preheat plateau tests carried out on sample IEE215 and IEE228 (see Supplementary data #1). The preheating prior to measurement of T_i was selected to be 220°C for 5 s based on the previous behavioral studies (Wang et al., 2006).

Sensitivity correction

Three samples (IEE211, IEE228 and IEE232) were used to test the ability of the new protocol to correct for sensitivity changes. Both additive and regenerative dose–response curves were constructed for these samples. Figure 2 presents these results and their combined dose–response curve obtained by the Australian slide method (Prescott et al., 1993) both with and without (insets of Fig. 2) sensitivity correction. The sensitivity-

corrected regenerated OSL dose–response curves for the two older samples (IEE228 and IEE232) are similar to those shown by Watanuki et al. (2003) for their quartz, obtained using a similar chemical treatment to remove feldspars. For these three samples, the regenerated OSL dose–response curve can be shifted to lie on top of that of the additive dose only when using the OSL response to the test dose to correct for sensitivity changes. Sample IEE211 shows only slight sensitivity change between the additive and regenerative curves for the raw data (see inset of Fig. 2a); however, for samples IEE228 and IEE232 large sensitivity changes can be seen in the inset of Figure 2b and c, respectively. Without using the test dose to monitor the sensitivity changes, only sample IEE211 can give a reasonable D_c determination by the slide method (inset of Fig. 2a), and no concordance between additive and regenerated dose–response can be found for sample IEE232 (inset of Fig. 2c). This indicates that no reliable D_c value can be obtained using the Australian slide method when OSL signals near saturation and using uncorrected OSL intensities for old samples.

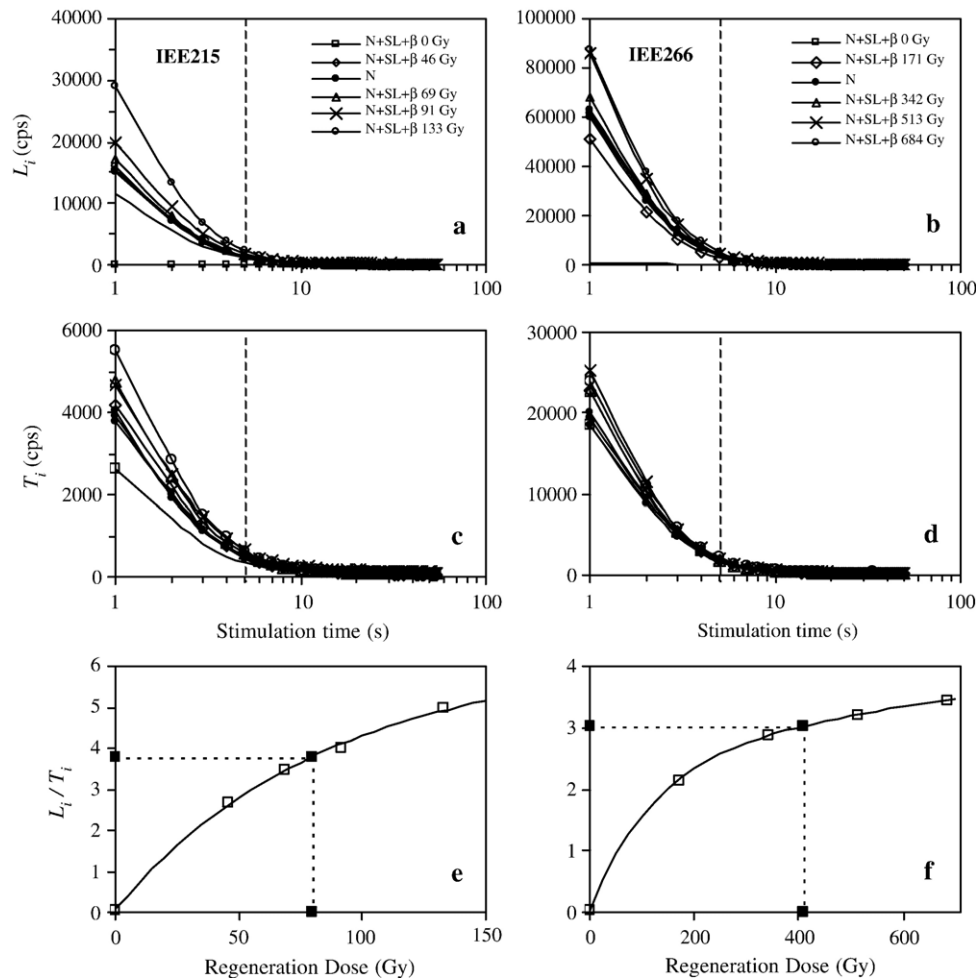


Figure 1. Representative data of D_e determination for two samples (IEE215 and IEE266) by the sensitivity-corrected MAR protocol. (a, b) Decay curves of natural and regeneration dose OSL intensity (L_i); (c, d) decay curves of test dose OSL intensity (T_i) after each natural and regenerative OSL measurement; (e, f) the corrected OSL (L_i/T_i) dose–response curves and D_e determination. The preheating condition is 260°C for 10 s for the regenerated dose, and 220°C for 5 s for the test dose OSL measurements. OSL signals were for the first 5 s of stimulation time, integrating the region to the left of the dashed vertical lines in panels a, b, c and d.

The dose–response curves constructed by the Australian slide method look harmonious after inter-aliquot normalization, even though sensitivity changes had occurred and there was considerable scatter of the raw OSL data (e.g., for sample IEE232 in the inset of Fig. 2c). This means that both additive and regenerative growth curves have the same pattern of OSL growth with dose after removing the effects of sensitivity change and they can be merged into one consistent dose–response curve. The intersection of the corrected natural OSL intensity with the slide dose–response curve confidently proves the validity of this method for D_e determination. Besides being able to accurately recover the D_e value, it is also necessary to be able to obtain it with high precision. Even for such uniform aliquots as are obtained using fine-grained quartz, individual measurements of the natural OSL intensity have a standard error of $\sim 1.5\%$. Additional experiments (see Supplementary data #2) showed that the use of the OSL response to a test dose reduces scatter to $\sim 0.3\%$, as has also been proved in previous studies on loess (Zhou and Shackleton, 2001). A similar improvement in precision was reported by Jain et al. (2003) in their application of component-specific normalization for a multiple-aliquot

protocol for fine-sand-sized grains of quartz from fluviually transported sands.

Comparison with the SAR protocol

The Single-Aliquot Regenerative-dose (SAR) procedure (Murray and Wintle, 2000) was applied to 23 of the 33 samples from the Heimugou section. The same preheat conditions were used as in the sensitivity-corrected MAR measurements, i.e., 260°C for 10 s for L_i measurements and 220°C for 5 s for the T_i measurements. Figure 3 shows that the D_e values determined by both the SAR and sensitivity-corrected MAR protocols are in good agreement for samples of last glacial loess, with D_e values less than 120 Gy (shown with an expanded scale in the upper inset of Fig. 3). However, the values of D_e obtained by the SAR protocol show unexpected underestimation; the maximum underestimation is 13% for the oldest sample IEE263, but the average amount of underestimation is about 8% for the last interglacial paleosol samples ($D_e > \sim 250$ Gy).

An experiment was designed to investigate whether this deviation between the SAR and sensitivity-corrected MAR data

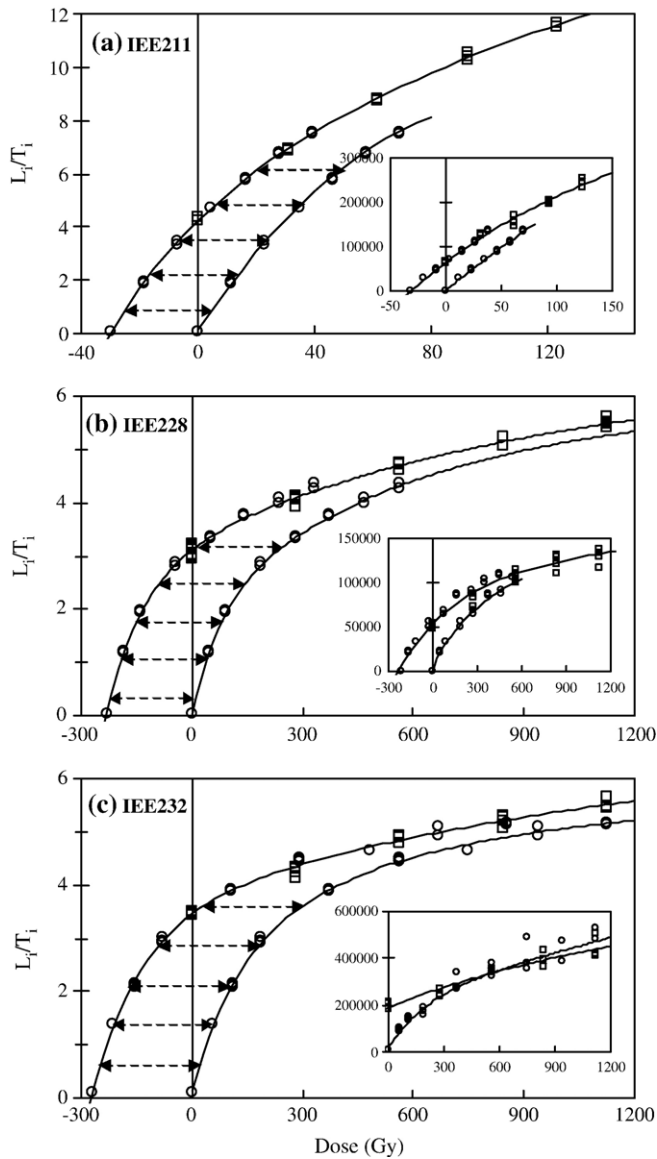


Figure 2. The additive (\square), regenerative dose (\circ) and their combined (Australian slide method) dose–response curves constructed using the corrected OSL intensity (L_i/T_i); the insets show the response of raw OSL intensity (L_i). The dose–response curves were fitted using the combination of two-exponential functions. Data for 3 samples: (a) IEE211 of Holocene age, and IEE228 (b) and IEE232 (c), above and below the S_1/L_1 transition, respectively.

sets could be the result of build up of an OSL signal during the repeated cycles of the SAR protocol, as had been suggested by Murray and Wintle (2003). The results (see Supplementary data #3) confirm a fundamental deviation in response of the signals, resulting in an 8% underestimation of SAR ages for regeneration doses of 400 Gy (see lower inset in Fig. 3). This is caused by the use of blue light stimulations in the SAR protocol, rather than the use of the broader and more powerful spectrum of the SOL2 sunlamp used in the sensitivity-corrected MAR protocol. This conclusion is supported by dose recovery test experiments when using different preheating conditions before OSL measurements of test dose (Wang et al., 2006). Thus, the sensitivity-corrected MAR protocol avoids OSL buildup during repeated measurements on single aliquot, as

only L_i and T_i are measured for each aliquot. An alternative approach would be to use a SAR protocol that employs optical stimulation between each measurement cycle (Murray and Wintle, 2003); however, this option was not explored here.

Dose rate determination

For all samples, Neutron Activation Analysis (NAA) was used to measure the uranium and thorium concentrations, and K content was determined by flame spectrum analysis (Table 1). The concentrations down-section are shown in Figure 4. The α efficiency factors, α values, were measured for each sample by comparing the OSL signals regenerated by α and β irradiation after an initial exposure to the SOL2 solar simulator for 3 min, as introduced by Zhou et al. (1995) for TL dating. The average value of α efficiency for all the samples is 0.045 ± 0.001 , consistent with values given by Rees-Jones (1995) for fine-grained quartz OSL.

It is also essential to determine the in situ water content. The weights of wet samples were measured immediately after extraction from the fresh section, and the dry samples were weighed after storing in an oven at 105°C for 8 h; combining these measurements we obtained the percentage water content (calculated as $[\text{wt water/wt dry sediment}] \times 100$) for this loess–paleosol sequence (Fig. 4). It is worth noting that the wetness reached its maximum at around the S_1/L_1 transition and its minimum in the upper part of L_{1-1} and L_{1-3} , shown by arrows in Figure 4. Based on the measured water contents, the average wetness for each layer is given in Table 1. The wetness may have varied slightly throughout burial time, but as the overburden increases the fluctuation will be small; an error of $\pm 2\%$ was thus assumed for all samples.

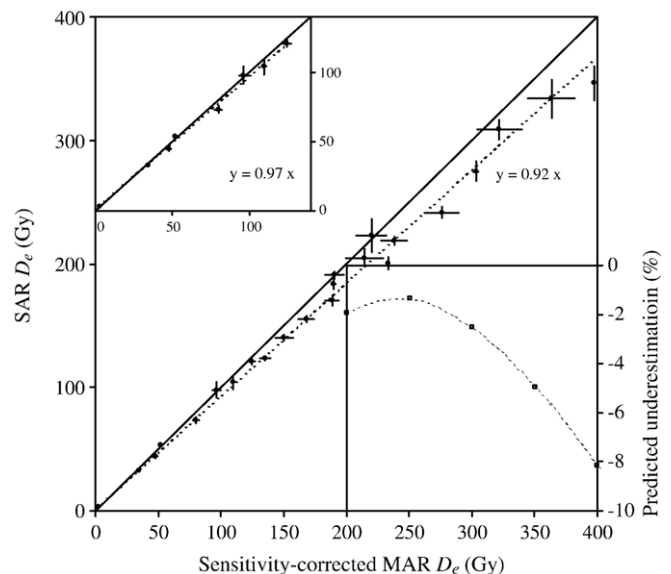


Figure 3. D_e comparison between SAR and sensitivity-corrected MAR protocols. The sensitivity-corrected MAR D_e values agree with those of the SAR protocol when D_e values are less than 120 Gy (see upper inset); SAR D_e values underestimate by an average of 8% for the older paleosol samples. The underestimation from 200 to 400 Gy is taken from the large data set in Fig. #2 of Supplementary data #3.

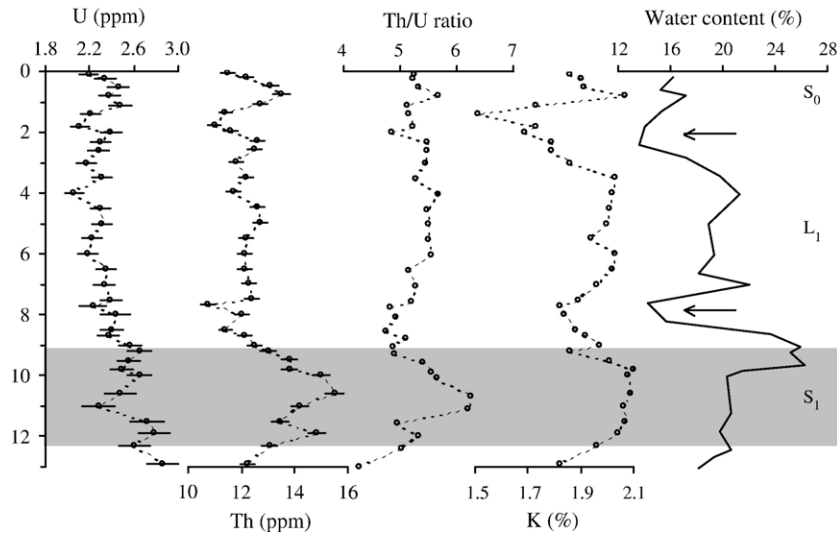


Figure 4. Related parameters for dosimetry of loess L₁ and paleosol S₁ (shaded); those include the concentrations of uranium, thorium, potassium and the measured water contents, as discussed in the text and given numerically in Table 1. Arrows show sediment layers with lowest water contents.

The dose rate for each loess sample is calculated directly by using the observed radionuclide concentrations and the water contents given in Table 1; the dose rates for the paleosol samples were corrected by using an empirical model (see Supplementary data #4), in which the dose rate is considered over two time periods: one is the time period with changing radiation conditions when S₁ was developing and serious weathering occurred, and the other is with relatively stable radiation environments after S₁ had been covered by the loess layer. In Table 1, the corrected dose rates for the S₁ paleosol samples, at depths of 9.5–11.9 m, were used for OSL age calculation.

Results and discussions

Comparison with relative independent age estimates

From the methodological studies, the sensitivity-corrected MAR protocol shows good performance in respect of sensitivity correction, overcoming the scatter of experimental data and avoiding the effects of buildup of OSL signals. Table 1 gives D_e values for all the samples. However, the best test of this new protocol is to compare the age estimates with independently derived ages. For the Luochuan loess–paleosol sequence, the S₁/L₁ transition offers a reference age for validating the sensitivity-corrected MAR protocol.

Previous studies have shown that the S₁/L₁ transition occurs at around 73.9±2.6 ka (SPECMAP age, Martinson et al., 1987), corresponding to the transition of MIS 5/4 that was confirmed by TL dating (Lu et al., 1987, 1988, 1999; Forman, 1991) and also by climate correlation (e.g., An and Lu, 1984; Liu, 1985; Porter and An, 1995; An and Porter, 1997). Two loess OSL ages for samples above this transition at Heimugou section have been obtained by the sensitivity-corrected MAR protocol; they are 71.1±3.4 (IEE229) and 70.4±2.6 ka (IEE230) (Fig. 5 and Table 1), consistent with

the reference age of 73.9±2.6 ka for MIS 5/4 in the SPECMAP record. The OSL age estimates beneath the S₁/L₁ transition (Fig. 5 and Table 1) also agree broadly with the ages expected for a soil formed in MIS 5. Thus, the sensitivity-corrected MAR protocol and the related experimental conditions are suitable, and age underestimation is not apparent for the loess L₁ at Luochuan on the Chinese Loess Plateau.

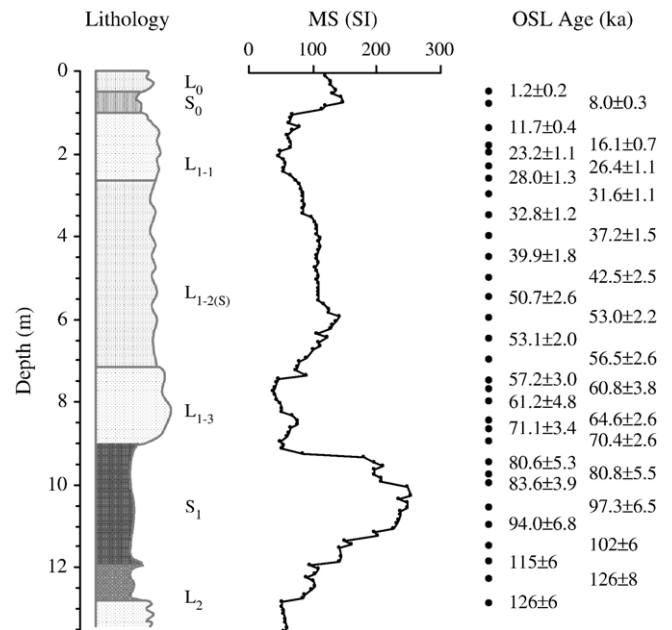


Figure 5. OSL ages (ka) obtained using the sensitivity-corrected MAR protocol on fine-grained quartz for Luochuan loess–paleosol units of the past 130 ka. The climato-stratigraphy at Luochuan is divided into L₀, S₀, L₁₋₁, L_{1-2(s)}, L₁₋₃, S₁ and L₂ according to the field observations and climato-environmental proxies (An and Lu, 1984). Low frequency magnetic susceptibility (MS) values were measured using a Bartington MS-2 magnetic susceptibility meter in the laboratory.

OSL chronology for Luochuan loess in the last glacial–interglacial period

Figure 5 and Table 1 present the sensitivity-corrected MAR OSL ages for the loess–paleosol sequence of S_1 , L_1 and S_0 units in the Heimugou section at Luochuan. The quartz OSL age estimates are stratigraphically consistent and no reversals occur (within measurement uncertainties). Our OSL ages of samples from the transition of L_2/S_1 and S_1/L_1 show that paleosol S_1 started about 126 ka and ended about 80 ka; this indicates that sedimentary quartz grains were deposited throughout the last interglacial, corresponding to the whole of MIS 5.

Our new chronology for the last glacial loess, L_1 , enables us to investigate the validity of the subdivision of this loess into three subunits (L_{1-1} , $L_{1-2(S)}$ and L_{1-3}), which was first proposed by An and Lu (1984) on the basis of field observations and climato-environmental proxies, such as magnetic susceptibility, grain size, $CaCO_3$ contents and soil micro-morphologic properties. They identified a weakly developed paleosol ($L_{1-2(S)}$) and then made a correlation to the marine isotope record, suggesting that the $L_{1-2(S)}$ paleosol was formed in MIS 3. In 1999, Lu et al. obtained an age of $\sim 30 \pm 2$ ka for this termination of the $L_{1-2(S)}$ in North China. This age seems not to be consistent with that of 24.1 ± 5.0 ka for the MIS 3/2 transition from the SPECMAP record (Martinson et al., 1987), but it is consistent with the proposed calendar age of 29 cal ka that is widely used (e.g., Voelker and Workshop participants, 2002).

In the current study, the boundary between $L_{1-2(S)}$ and L_{1-1} occurs between samples IEE217 dated to 28.0 ± 1.3 ka and IEE218 dated to 31.6 ± 1.1 ka, giving an age estimate of about 29.3 ± 1.5 ka (Table 1). This is also in good agreement with the implication of the ^{230}Th age of 31.9 ± 0.4 ka for the final marine high-stand of MIS 3, recorded by terraces in New Guinea (Shackleton et al., 2004). The lower boundary of the weak paleosol ($L_{1-3}/L_{1-2(S)}$) is found to have an estimated age of 57.0 ± 3.8 ka, between sample IEE226 dated to 56.5 ± 2.6 ka and IEE227 dated to 57.2 ± 3.0 ka. These results fundamentally agree with the age of 59.0 ± 5.6 ka for the MIS 4/3 transition (Martinson et al., 1987) and the proposed calendar age of 59 cal ka (Voelker and Workshop participants, 2002). Thus, the grains making up the weakly developed paleosol, $L_{1-2(S)}$, began to be deposited at about 57 ka and ended at about 29 ka (Fig. 5). Thus, the subunits of L_{1-1} , $L_{1-2(S)}$ and L_{1-3} can be correlated to MIS 2, 3 and 4, respectively, supporting the previous climato-chronostratigraphy (An and Lu, 1984).

Implication for dust accumulation rates in the last 70 ka

One of the advantages of OSL dating is that the ages obtained represent the last sunlight exposure event before deposition; thus, our OSL ages are helpful in depicting the dust deposition in the last glacial. Dust accumulation at Luochuan appears to have been continuous for the period between 74 and 12 ka, and we have attempted to regress the sample depths against their associated OSL ages to calculate accumulation rates. During this period of time, there have

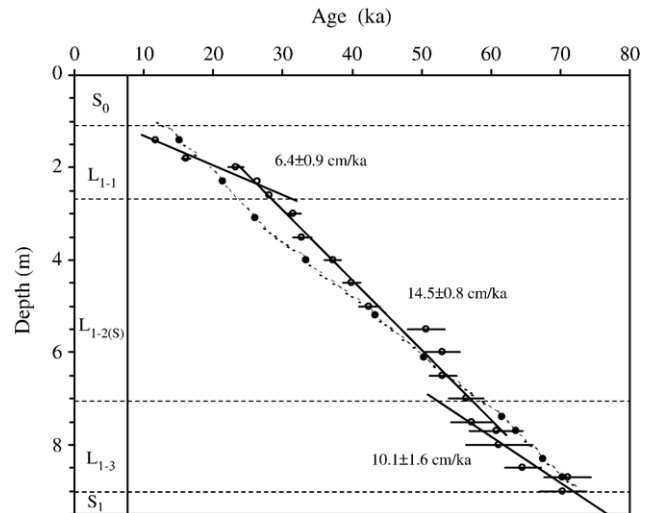


Figure 6. Relationship between the OSL age (O) and depth for samples from the Heimugou section at Luochuan during the last 72–12 ka. The regression lines show three periods with different dust accumulation rates (6.4 ± 0.9 , 14.5 ± 0.8 and 10.1 ± 1.6 cm/ka for L_{1-1} , $L_{1-2(S)}$ and L_{1-3} , respectively) as shown by the solid lines. The grain-size modeling ages are shown by the dashed line with data (●) taken from Table 1 of Porter and An (1995) for the Potou section at Luochuan. The divisions related to the lithostratigraphy of An and Lu (1984) are also shown.

been changes in the accumulation rate, and the rates are shown in Figure 6. It can be seen that there is a relatively low accumulation rate for L_{1-3} in the period from ~ 72 to ~ 57 ka, corresponding to MIS 4. The accumulation rate increases at the $L_{1-3}/L_{1-2(S)}$ boundary from 10.1 ± 1.6 cm/ka to 14.5 ± 0.8 cm/ka, though the age of 50.7 ± 2.6 ka for sample IEE223 seems a little high in relation to the trend line. At $\sim 28 \pm 2$ ka the accumulation rate decreases to the lowest value for the last 70 ka, namely 6.4 ± 0.9 cm/ka. This change at 28 ± 2 ka is basically consistent with the timing of the MIS 3/2 boundary. However, it is clear that a high average accumulation rate occurred in the last interstadial paleosol ($L_{1-2(S)}$), corresponding to MIS 3, not in the classic L_{1-1} and L_{1-3} loess of the cold-dry glacial condition (MIS 2 and 4).

These results disagree with the previous estimates of the accumulation rate in the Luochuan area (site name: Heimugou_1/Luochuan in Table 2 of Kohfeld and Harrison, 2003) and also with the average accumulation rates on the Chinese Loess Plateau (Fig. 10 of An, 2000), as shown in Table 2. These previously published accumulation rates (An, 2000; Kohfeld and Harrison, 2003) were calculated on the basis of very few absolute dates or a relative time scale linked to the SPECMAP record through the climato-stratigraphic subdivisions of An and Lu (1984). In those studies, the accumulation rates were reported to be relatively high during MIS 2 and 4. It is suspected that the previous studies excessively stressed the dust supply in relatively cold and dry conditions. In fact, the surface condition is also one of the important factors controlling dust accumulation on the Chinese Loess Plateau. It is possible that the improved vegetation cover in the last interstadial (Jiang and Ding, 2005) helped dust entrapment on the Chinese Loess Plateau.

Table 2

Accumulation rates (cm/ka) in Luochuan area for lithostratigraphic units L_{1-1} (28–12 ka), $L_{1-2(S)}$ (57–28 ka) and L_{1-3} (72–57 ka) based on OSL ages and for MIS 2 (24–12 ka), 3 (60–24 ka) and 4 (72–60 ka) from Fig. 10 of An (2000) and Table 2 of Kohfeld and Harrison (2003)

Time period (ka)	Depth (m)	OSL based	An (2000)	Kohfeld and Harrison (2003) ^a
24–12 (MIS 2)			15.5	18.5
28–12 (L_{1-1})	1.4–2.6	6.4±0.9		16.9
60–24 (MIS 3)			9.7	8.4
57–28 ($L_{1-2(S)}$)	2.6–7.0	14.5±0.8		6.6
72–60 (MIS 4)			15.8	19
72–57 (L_{1-3})	7.5–9.0	10.1±1.6		14.5

^a Kohfeld and Harrison (2003) reported the mass accumulation rates, based on two different magnetic susceptibility records at Heimugou, and used a bulk density of 1.48 g/cm³.

Comparison with “grain-size modeling” ages

Having obtained a tight chronology using the sensitivity-corrected MAR protocol, we feel sufficiently confident to look at its implication for the “grain-size model” proposed by Porter and An (1995) for derivation of a chronology for the Chinese loess–paleosol succession. They assumed that the dust flux during the last glacial period varied with changing climate, and that the dust flux was proportional to grain size. Porter (2001) has claimed that ages based on this model are reliable, with calculated errors ranging from ±1 to 3 ka. The core issue in the grain-size model concerns the assumed relationship between grain size and dust flux. Figure 6 also presents the results of grain-size modeling ages from Table 1 of Porter and An (1995) for the Potou section, 2 km west of the Heimugou section studied here. Their results suggest that dust accumulation at Luochuan was effectively continuous and constant for the whole of the period from 74 ka to 12 ka. This conflicts with our results, based on OSL ages, which show that, although deposition appears to be continuous, two changes in the dust accumulation rate occurred within the same period at ~57 (or ~60) ka and ~28 (or ~24) ka. Thus, it is strongly recommended that the basic premise of the “grain-size” model should be checked, as this is the most likely reason for the discrepancy in the chronology between 40 ka and 16 ka seen in Figure 6.

Conclusion

A sensitivity-corrected MAR protocol is proposed to determine fine-grained quartz OSL ages for Chinese loess at one intensively studied section. From the methodological viewpoint, the sensitivity-corrected MAR protocol can correct for sensitivity changes that occur during the measurement process, overcome the scatter of the experimental data in MAR measurement procedures and avoid the buildup of OSL signals that happens in the SAR protocol. This has enabled us to recover D_e values with high accuracy and precision. When comparing the OSL ages obtained in this way with the reference age (73.9±2.6 ka) of the MIS 5/4 transition

recorded at the S_1/L_1 boundary, no age underestimation is apparent.

Based on the closely spaced samples extracted from the Heimugou section, a new OSL chronostratigraphy is reported for the last glacial loess in the Luochuan area on the Chinese Loess Plateau. Changes in the accumulation rate have occurred twice in the period from 74 ka to 12 ka, one at a time of about 57±3.8 ka of $L_{1-3}/L_{1-2(S)}$ boundary, corresponding to the MIS 4/3 transition, and the other at about 28±2 ka, close to $L_{1-2(S)}/L_{1-1}$ transition (MIS 3/2).

Compared with previously published results, it is clear that the average accumulation rate is higher in the last interstadial paleosol ($L_{1-2(S)}$), corresponding to MIS 3, than in the classic L_{1-1} and L_{1-3} loess of the cold-dry glacial condition (MIS 2 and 4). Also, comparing our results with the numerical chronology obtained using a published grain-size model, it seems that the assumption of a direct relationship between grain size and dust flux may be in question.

Acknowledgments

We thank Prof. Z.S. An (Institute of Earth Environment, CAS) for scientific comments and support. We are grateful to the two referees for suggestions that have improved the manuscript substantially. This work was funded by CNSF (40602020, 40523002) and National Basic Research Program of China (No: 2004CB720201).

Appendix A. Supplementary data

Supplementary data associated with this article can be found in the online version at doi:10.1016/j.yqres.2006.08.003.

References

- Aitken, M.J., 1998. An Introduction to Optical Dating. Oxford University Press, Oxford, p. 267.
- An, Z.S., 2000. The history and variability of the East Asian paleomonsoon climate. Quaternary Science Reviews 19, 171–187.
- An, Z.S., Lu, Y.C., 1984. A climatostratigraphic subdivision of Late Pleistocene strata named by Malan formation in North China. Chinese Science Bulletin 29, 1239–1242.
- An, Z.S., Porter, S.C., 1997. Millennial-scale climatic oscillations during the last interglaciation in central China. Geology 25, 603–606.
- An, Z.S., Liu, T.S., Lu, Y.C., Porter, S.C., Kukla, G., Wu, X.H., Hua, Y.M., 1990. The long term paleomonsoon variation recorded by the loess–paleosol sequence in central China. Quaternary International 7/8, 91–95.
- Bronger, A., 2003. Correlation of loess–paleosol sequences in East and Central Asia with SE Central Europe: Towards a continental Quaternary pedostratigraphy and paleoclimatic history. Quaternary International 106/107, 11–31.
- Forman, S.L., 1991. Late Pleistocene chronology of loess deposition near Luochuan, China. Quaternary Research 36, 19–28.
- Frechen, M., 1999. Luminescence dating of loessic sediments from the Loess plateau, China. Geologische Rundschau 87, 675–684.
- Huntley, D.J., Godfrey-Smith, D.I., Thewalt, M.L.W., 1985. Optical dating of sediments. Nature 313, 105–107.
- Jain, M., Bøtter-Jensen, L., Singhvi, A.K., 2003. Dose evaluation using multiple-aliquot quartz OSL: Test of methods and a new protocol for improved accuracy and precision. Radiation Measurements 37, 67–80.
- Jiang, H.C., Ding, Z.L., 2005. Temporal and spatial changes of vegetation

- cover on the Chinese Loess Plateau through the last glacial cycle: Evidence from spore-pollen records. *Review of Palaeobotany and Palynology* 133, 23–37.
- Kohfeld, K.E., Harrison, S.P., 2003. Glacial–interglacial changes in dust deposition on the Chinese Loess Plateau. *Quaternary Science Reviews* 22, 1859–1878.
- Kukla, G., 1987. Loess stratigraphy in central China. *Quaternary Science Reviews* 6, 191–219.
- Kukla, G., An, Z.S., 1989. Loess stratigraphy in central China. *Palaeogeography, Palaeoclimatology, Palaeoecology* 72, 203–205.
- Kukla, G., Heller, F., Liu, X.M., Xu, T.C., Liu, T.S., An, Z.S., 1988. Pleistocene climates in China dated by magnetic susceptibility. *Geology* 16, 811–814.
- Liu, T.S. (Ed.), 1985. *Loess and the Environment*. China Ocean Press, Beijing.
- Lu, Y.C., Prescott, J.R., Robertson, G.B., Hutton, J.T., 1987. Thermoluminescence dating of the Malan loess at Zhaitang, China. *Geology* 15, 603–605.
- Lu, Y.C., Zhang, J.Z., Xie, J., 1988. Thermoluminescence dating of loess and paleosols from the Lantian section, Shaanxi Province, China. *Quaternary Science Reviews* 7, 245–250.
- Lu, Y.C., Zhao, H., Yin, G.M., Chen, J., Zhang, J.Z., 1999. Luminescence dating of loess–paleosol sequences in the past about 100 ka in North China. *Bulletin of the National Museum of Japanese History* 81, 209–220.
- Martinson, D.G., Pisias, N.G., Hays, J.D., Imbrie, J., Moore, T.C., Shackleton, N.J., 1987. Age dating and the orbital theory of the ice ages: Development of a high-resolution 0 to 300,000 year chronostratigraphy. *Quaternary Research* 27, 1–29.
- Murray, A.S., Wintle, A.G., 2000. Luminescence dating of quartz using an improved single-aliquot regenerative-dose protocol. *Radiation Measurements* 32, 57–73.
- Murray, A.S., Wintle, A.G., 2003. The single aliquot regenerative dose protocol: Potential for improvements in reliability. *Radiation Measurements* 37, 377–381.
- Musson, F.M., Clarke, M.L., Wintle, A.G., 1994. Luminescence dating of loess from the Liujiapo section, central China. *Quaternary Science Reviews* 13, 407–410.
- Porter, S.C., 2001. Chinese loess record of monsoon climate during the last glacial–interglacial cycle. *Earth-Science Reviews* 54, 115–128.
- Porter, S.C., An, Z.S., 1995. Correlation between climate events in the North Atlantic and China during the last glaciation. *Nature* 375, 305–308.
- Prescott, J.R., Robertson, G.B., 1997. Sediment dating by luminescence: A review. *Radiation Measurements* 27, 893–922.
- Prescott, J.R., Huntley, D.J., Hutton, J.T., 1993. Estimation of equivalent dose in thermoluminescence dating—The Australian slide method. *Ancient TL* 11, 1–5.
- Rees-Jones, J. 1995. *Optical dating of selected British archaeological sediments*. Unpublished D. Phil. Thesis, University of Oxford.
- Roberts, H.M., Duller, G.A.T., 2004. Standardized growth curves for optical dating of sediment using multiple-grain aliquots. *Radiation Measurements* 38, 241–252.
- Rousseau, D.D., Wu, N.Q., 1997. A new molluscan record of the monsoon variability over the past 130,000 yr in the Luochuan loess sequence, China. *Geology* 25, 275–278.
- Shackleton, N.J., Fairbanks, R.G., Chiu, T.C., Parrenin, F., 2004. Absolute calibration of the Greenland time scale: Implications for Antarctic time scales and for $\Delta^{14}\text{C}$. *Quaternary Science Reviews* 23, 1513–1522.
- Voelker, A.H.L., and Workshop participants, 2002. Global distribution of centennial-scale records for Marine Isotope Stage (MIS) 3: A database. *Quaternary Science Reviews* 21, 1185–1212.
- Wang, X.L., Lu, Y.C., Zhao, H., 2006. On the performances of the single-aliquot regenerative-dose (SAR) protocol for Chinese loess: Fine quartz and polymineral grains. *Radiation Measurements* 41, 1–8.
- Watanuki, T., Murray, A.S., Tsukamoto, S., 2003. A comparison of OSL ages derived from silt-sized quartz and polymineral grains from Chinese loess. *Quaternary Science Reviews* 22, 991–997.
- Wintle, A.G., 1990. A review of current research on TL dating of loess. *Quaternary Science Reviews* 9, 385–397.
- Wintle, A.G., 1997. Luminescence dating: Laboratory procedures and protocols. *Radiation Measurements* 27, 769–817.
- Xiao, J.L., An, Z.S., Liu, T.S., Inouchi, Y., Kumai, H., Yoshikawa, S., Kondo, Y., 1999. East Asian monsoon variation during the last 130,000 years: Evidence from the Loess Plateau of central China and Lake Biwa of Japan. *Quaternary Science Reviews* 17, 147–157.
- Zhao, H., 2003. Comparison of dating results between polymineral fine grains SAR and MAR. *Nuclear Techniques* 26, 36–39 (In Chinese with English abstract).
- Zhou, L.P., Shackleton, N.J., 2001. Photon-stimulated luminescence of quartz from loess and effects of sensitivity change on palaeodose determination. *Quaternary Science Reviews* 20, 853–857.
- Zhou, L.P., Wintle, A.G., 1994. Sensitivity change of thermoluminescence signals after laboratory optical bleaching: Experiments with loess fine grains. *Quaternary Science Reviews* 13, 457–463.
- Zhou, L.P., Dodonov, A.E., Shackleton, N.J., 1995. Thermoluminescence dating of the Orkutsay loess section in Tashkent region, Uzbekistan, Central Asia. *Quaternary Science Reviews* 14, 721–730.